

Applications of AUSM+ Scheme on Subsonic, Supersonic and Hypersonic Flows Fields

Muhammad Yamin Younis¹, Muhammad Amjad Sohail², Tawfiqur Rahman³, Zaka Muhammad⁴,
Saifur Rahman Bakaul⁵

Abstract—The performance of Advection Upstream Splitting Method AUSM schemes are evaluated against experimental flow fields at different Mach numbers and results are compared with experimental data of subsonic, supersonic and hypersonic flow fields. The turbulent model used here is SST model by Menter. The numerical predictions include lift coefficient, drag coefficient and pitching moment coefficient at different mach numbers and angle of attacks. This work describes a computational study undertaken to compute the Aerodynamic characteristics of different air vehicles configurations using a structured Navier-Stokes computational technique. The CFD code bases on the idea of upwind scheme for the convective (convective-moving) fluxes. CFD results for GLC305 airfoil and cone cylinder tail finned missile calculated on above mentioned turbulence model are compared with the available data. Wide ranges of Mach number from subsonic to hypersonic speeds are simulated and results are compared. When the computation is done by using viscous turbulence model the above mentioned coefficients have a very good agreement with the experimental values. AUSM scheme is very efficient in the regions of very high pressure gradients like shock waves and discontinuities. The AUSM versions simulate the all types of flows from lower subsonic to hypersonic flow without oscillations.

Keywords—Subsonic, supersonic, Hypersonic, AUSM+, Drag Coefficient, lift Coefficient, Pitching moment coefficient, pressure Coefficient, turbulent flow.

I. INTRODUCTION

AUSM stands for Advection Upstream Splitting Method. It is developed as a numerical inviscid flux function for solving a general system of conservation equations and especially it is used to simulate hyperbolic conservation equations. It is based on the upwind concept and was motivated to provide an alternative approach to other upwind methods, such as the Godunov method, flux difference splitting methods by Roe, and Solomon and Osher, flux vector splitting methods by Van Leer, and Steger and Warming. The AUSM first recognizes that the inviscid flux consist of two physically distinct parts, i.e., convective and pressure fluxes. The former is associated with the flow (advection) speed, while the latter with the acoustic speed; or respectively classified as the linear and nonlinear fields. Currently, the convective and pressure fluxes are formulated using the

eigenvalues of the flux Jacobian matrices. The method was originally proposed by Liou and Steffen [1] for the typical compressible aerodynamic flows and they implemented it successfully for discontinuous flows, and later these schemes are substantially improved [2,3] to yield a more accurate and robust version. To extend its capabilities, it has been further developed in [4-6] for all speed-regimes from low subsonic, subsonic, transonic, supersonic and hypersonic flows with and without discontinuities and multiphase flow and for combustion and mixing flows. Its variants have also been proposed [7,8] and implemented for different types of flows. The Advection Upstream Splitting Method has many features. The main features are:

- accurate capturing of shock and contact discontinuities
- entropy-satisfying solution
- positivity-preserving solution
- algorithmic simplicity (not requiring explicit eigen-structure of the flux Jacobian matrices) and straightforward extension to additional conservation laws
- free of “carbuncle” phenomena
- Uniform accuracy and convergence rate for all Mach numbers.

Since the method does not specifically require eigenvectors, it is especially attractive for the system whose eigen-structure is not known explicitly. The AUSM has been employed to solve a wide range of problems, low-Mach to supersonic and hypersonic aerodynamics [9, 10], large eddy simulation and aero-acoustics [11,12], direct numerical simulation [13], galactic relativistic flow[14]. In the present work AUSM scheme and its different version are used to simulate a wide variety of flow field from subsonic to hypersonic speed for different configurations and geometries. It is successfully applied and implemented for all types of flow fields. This scheme seems very powerful tool to simulate the high pressure flow fields having discontinuities and shocks. The configurations taken for this research work are GLC305 airfoil [15], cone cylinder body [16,17] and reentry vehicle cone probe[17].

First and second authors is with the Beijing University of Aeronautics and Astronautics China, phone: 0086-13120491221;; e-mail: masohailamer@yahoo.com).

Third to fifth authors are with the Beijing University of Aeronautics and Astronautics China department 15 , phone: 0086-13661303504;; e-mail: masohailamer@yahoo.com).

II. GEOMETRICAL MODELS

The subsonic GLC305 [15] airfoil is used here to simulate its different cases of Mach number and Reynolds numbers. The supersonic projectile model in this study is a basic finned;

a cone-cylinder-finned configuration and cone cylinder body (see Figure1). The length of the projectile without fins is 6 calibers and the diameter is 40 mm. the length of fined body is 10 calibers and diameter is 30 mm. Four fins are located on the back end of the projectile. All necessary details of geometries are given in reference [16,17]. A hypersonic reentry cone probe [18] is simulated at mach 5.9 and its tip to base radius ratios is changed from 0.025 and 0.50 and angle of cone is taken 30° . A structured computational mesh was generated for these configurations. In general, most of the grid points are clustered in the near wall region to capture the boundary layer and control the Y^+ value for turbulence model.

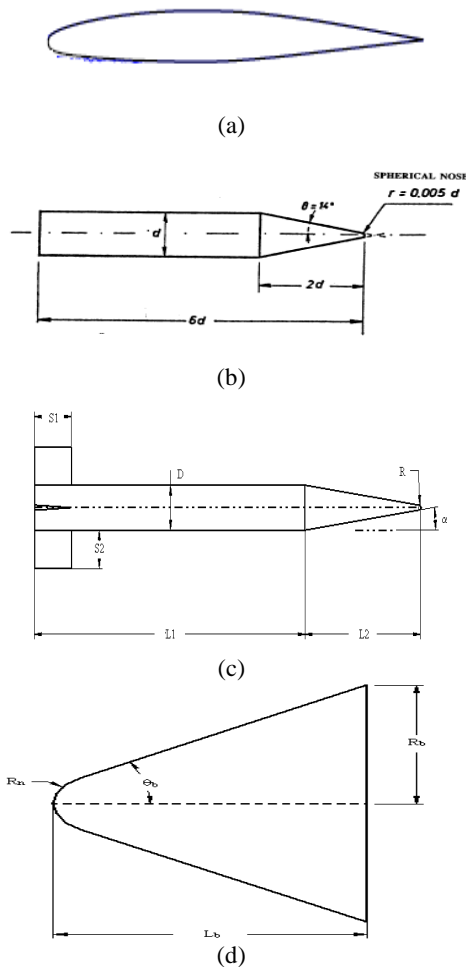


Fig. 1 (a) airfoil (b)(c) cone cylinder with and without fins (d) cone

III. GOVERNING EQUATIONS AND NUMERICAL METHOD

The system of governing equations for a single-component fluid, written to describe the mean flow properties, is cast in integral Cartesian form for an arbitrary control volume V with differential surface area dA as follows:

$$\frac{\partial}{\partial t} \int_V W dV + \oint [F - G] dA = \int_V H dV \quad (1)$$

Where the vectors W , F and G are defined as:

$$W = \begin{bmatrix} \rho \\ \rho u \\ \rho v \\ \rho w \\ \rho E \end{bmatrix}, F = \begin{bmatrix} \rho u \\ \rho v u + P \hat{i} \\ \rho v v + P \hat{j} \\ \rho v w + P \hat{k} \\ \rho v E + P v \end{bmatrix}, G = \begin{bmatrix} 0 \\ \tau_{xi} \\ \tau_{yi} \\ \tau_{zi} \\ \tau_{ij} v_j + q \end{bmatrix}$$

Vector H contains source terms such as body forces and energy sources.

Here ρ , v , E , and p are the density, velocity, total energy per unit mass, and pressure of the fluid, respectively. T is the viscous stress tensor, and q is the heat flux.

Total energy E is related to the total enthalpy H by

$$E = H - p/\rho$$

Where

$$H = h + |v|^2/2$$

IV. NUMERICAL METHODS

4.1 Advection Upstream Splitting Method

The Advection Upstream Splitting Method (AUSM) scheme was introduced and applied by Liou and Steffen in 1991 [1-3]. The AUSM scheme defines a cell interface Mach number based on characteristic speeds from the neighboring cells. The interface Mach number is used to determine the upwind extrapolation for the convective part of the inviscid fluxes. A separate splitting is used for the pressure terms. Generalized Mach number and pressure splitting functions are described by Liou [1,2,4] and the new scheme was termed ASUM+. The AUSM+ scheme was shown to have several desirable properties:

1. It gives exact resolution of 1-D contact and shock discontinuities,
2. It preserves positivity of scalar quantities,
3. It is free of oscillations at stationary and moving shocks.

The AUSM+ scheme avoids an explicit artificial dissipation, and differences the fluxes directly using:

$$\partial_\xi E = E_{i+1/2} - E_{i-1/2}$$

The algebraic method is used to generate three-dimensional boundary-fitted grids for a cone. The height of the first grid next to the body is controlled, and the grids near to the body are normalized. The C-type mesh is generated on the tip of the cone. The grid size is 70x50x36 is used for this geometry.

V. TURBULENCE MODEL

The K- ω SST model [19,20] (Menter, 1993) is a two equation model that solves the transport of specific dissipation rate of turbulent kinetic energy and the turbulent kinetic energy. This model is a combination of the k - ω and k - ϵ models.

$$\frac{\partial}{\partial t}(\rho k) + \frac{\partial}{\partial x_j}(\rho u_j k) = p - C_{\mu} \rho a k + \frac{\partial}{\partial x_j} \left[(\mu + \sigma_k \mu_t) \frac{\partial k}{\partial x_j} \right] \quad (2)$$

$$\frac{\partial}{\partial t}(\rho \omega) + \frac{\partial}{\partial x_j}(\rho u_j \omega) = \frac{\gamma p}{\mu_t} p - \beta \rho \omega^2 + \frac{\partial}{\partial x_j} \left[(\mu + \sigma_{\omega} \mu_t) \frac{\partial \omega}{\partial x_j} \right] + (1 - F_1) 2 \rho \sigma_{\omega} \frac{1}{\omega} \frac{\partial k}{\partial x_j} \frac{\partial \omega}{\partial x_j} \quad (3)$$

A. 3.4 Steady-State Flow Solution Methods

The coupled set of governing equations is discretized in time for steady calculations. In the steady case, it is assumed that time marching proceeds until a steady-state solution is reached. Temporal Discretization of the coupled equations is accomplished by an explicit time-marching algorithm.

3.5 Explicit Formulation

A density based explicit formulation is used for these computations. In the explicit scheme a multi-stage, time-stepping algorithm^[21] is used to discretize the time derivative in Equation 1. The solution is advanced from iteration n to iteration n+1 with an m-stage Runge-Kutta scheme given by

$$\begin{aligned} Q^0 &= Q^n \\ \Delta Q^i &= -\alpha_i \Delta t \Gamma^{-1} R^{i-1} \\ Q^{n+1} &= Q^m \end{aligned} \quad (4)$$

VI. RESULTS AND DISCUSSION

4 Results and Discussion

In the figures 2-5 airfoil GLC305 pressure, density and velocity distributions contours are shown. The comparison of different aerodynamics characteristics against angle of attack for different Mach number is graphed.

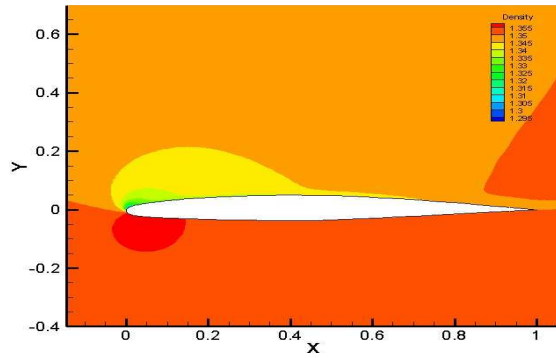
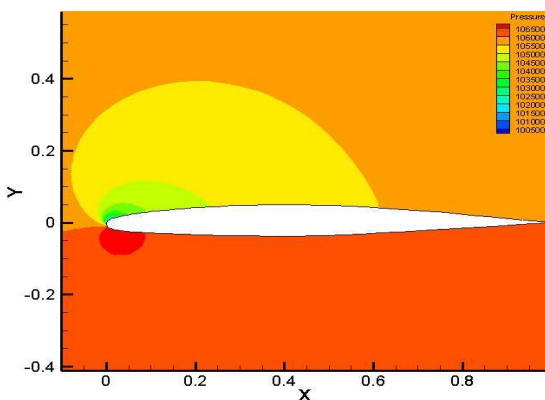


Fig. 2 (a) Pressure and density distribution on clean GLC305 at AoA = 8° M = 0.12, Re = 3x10⁶

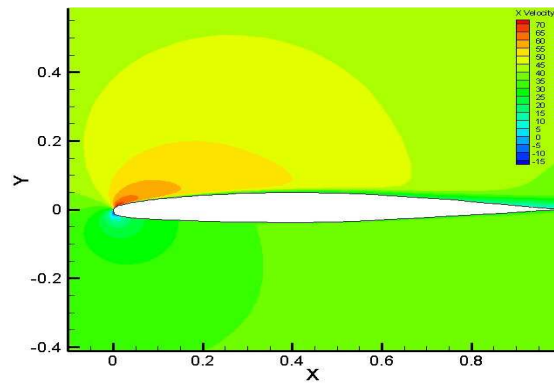


Fig. 2 (b) Velocity distribution on clean GLC305 at AoA = 8° M = 0.12, Re = 3x10⁶

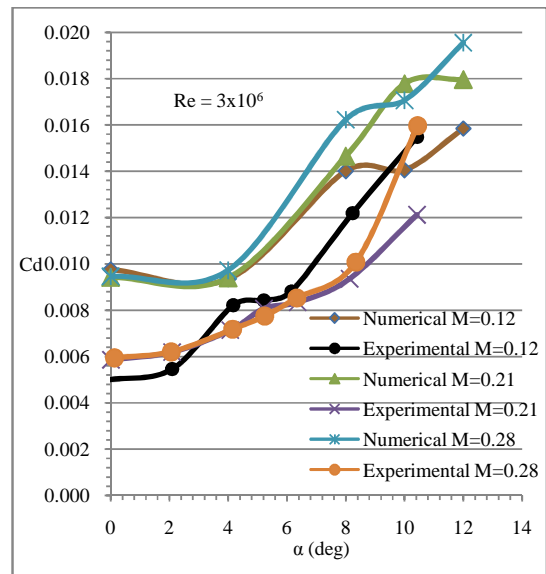


Fig. 3 Lift coefficient vs AoA for clean GLC305 airfoil

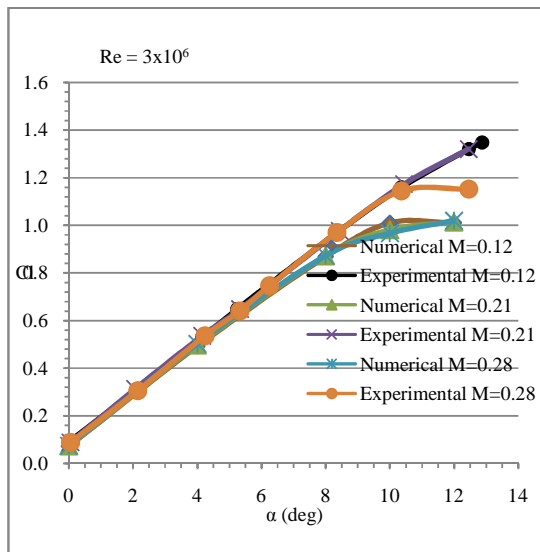


Fig. 4 Drag coefficient vs AoA for clean GLC305 airfoil

From figures 6 to 9 cone cylinder and cone cylinder with fins contours and graphs are plotted. The cone cylinder body configurations are simulated and mach 4 other test conditions are given in ref.16 and the finned missile [17] is simulated at different Mach number as shown in the graph. The results for AUSM scheme have a satisfactory agreement with the experimental and Roe scheme and other available data.

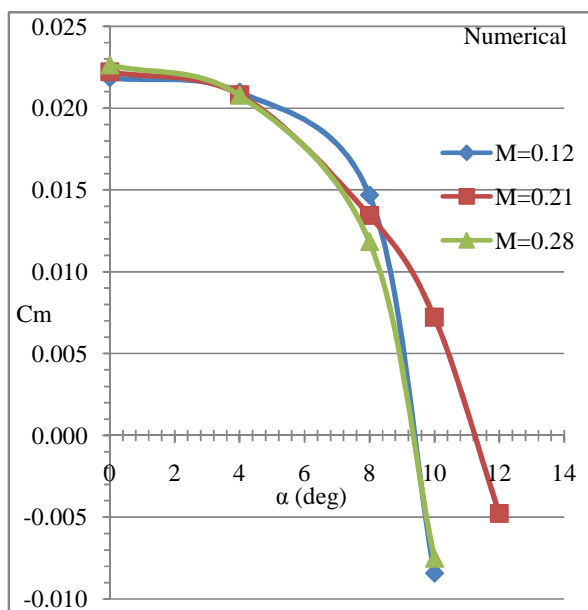


Fig. 5 Pitching moment coefficient vs AoA for clean GLC305 airfoil at different Mach number

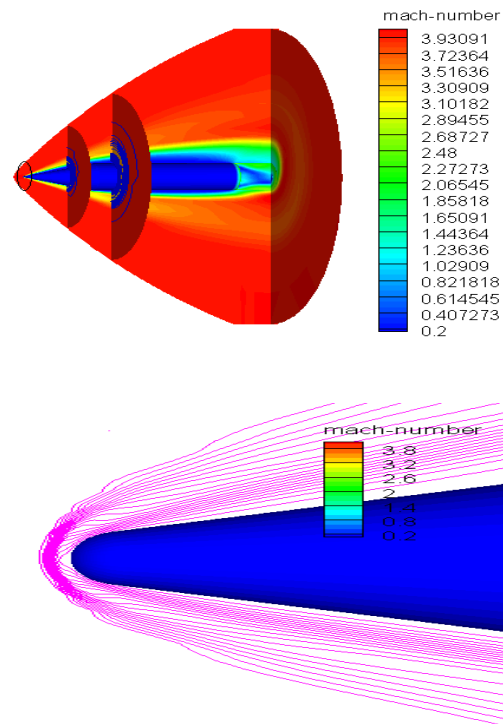


Fig. 6 Mach number contours for cone cylinder at mach 4 angle of attack 4°

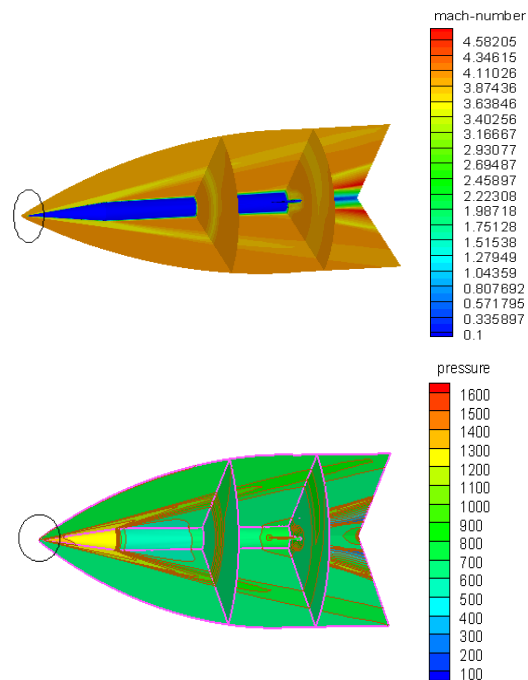


Fig. 7 Contours of Mach number and pressure for AUSM scheme at angle of attack 1°.

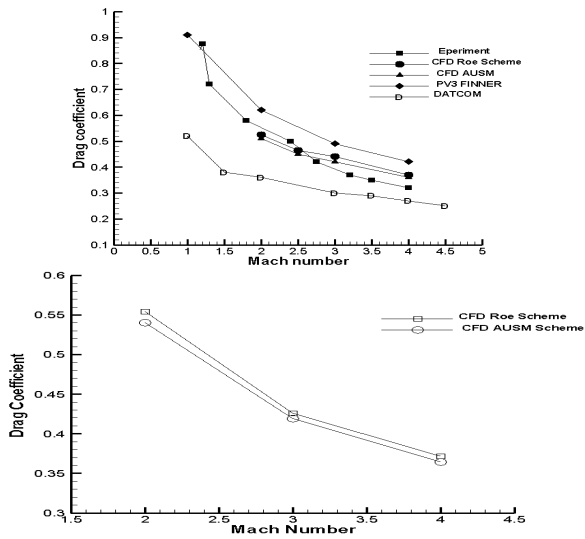


Fig. 8 Drag coefficient of finned missile at zero and 1° angle of attack.

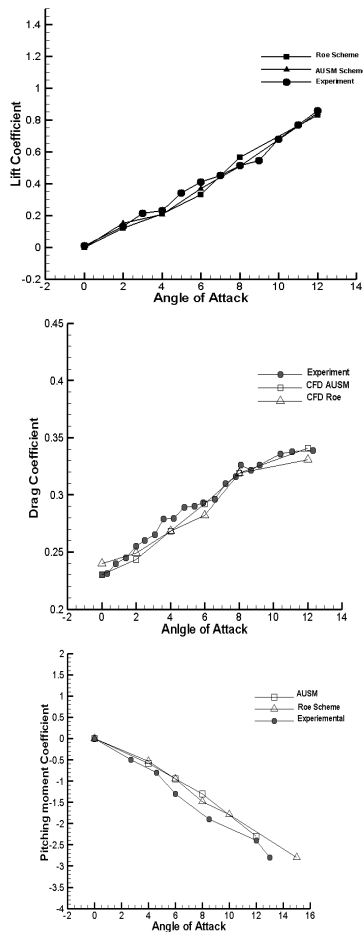


Fig. 9 Drag, lift and pitching moment coefficient of cone cylinder body against angle of attack.

From figure 10 to 15 contours of temperature, pressure,

Mach number and density are shown for different cone probe configurations. Shock waves are captured by this scheme very accurately as shown in figure. The results for drag lift and pitching moment coefficients have a very good agreement with the experimental results. For this hypersonic flow shock waves is captured by the AUSM scheme and the soluble is stable and got higher order accuracy by using limiters.

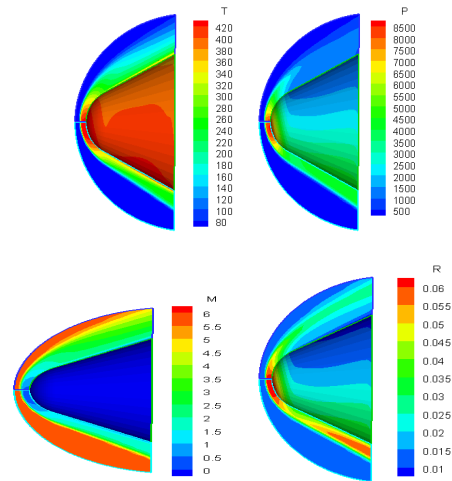


Fig. 10 Contours of temperature, pressure, mach no., and density at Mach 5.9, $r_n/r_b=0.5$ and angle of attack 12°

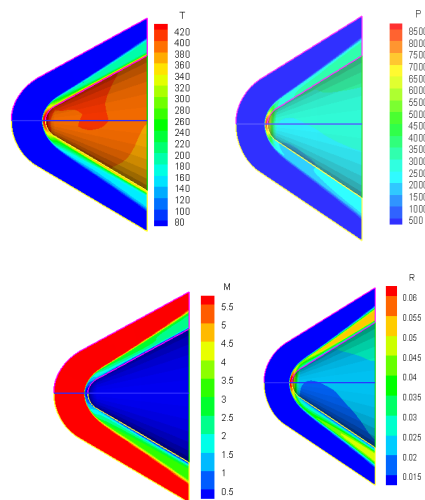


Fig. 11 Contours of Temperature, pressure, Mach no. and density at $\theta=30^\circ$, $r_n/r_b=0.25$ and angle of attack -4°

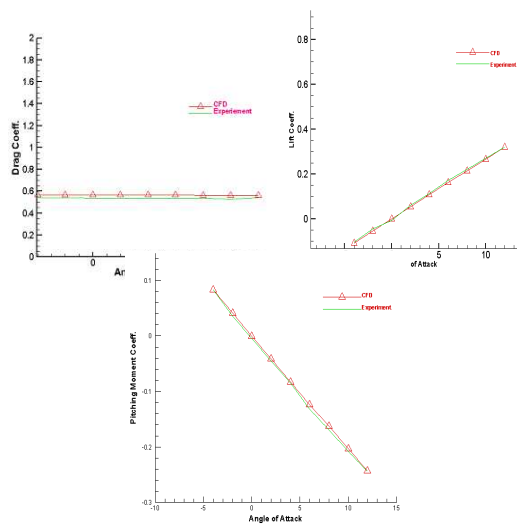


Fig. 13 Graph for Drag coeff. , lift and Pitching moment Coefficient for $r_n/r_b=0$ and $\theta=30^\circ$

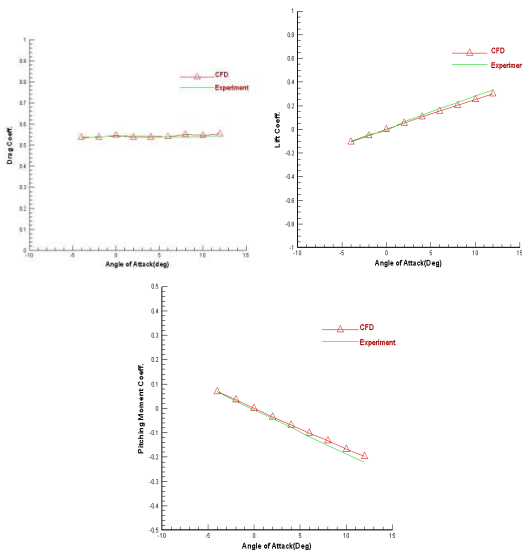


Fig. 14 Graph for Drag coeff. , lift and Pitching moment Coefficient for $r_n/r_b=0.25$ and $\theta=30^\circ$

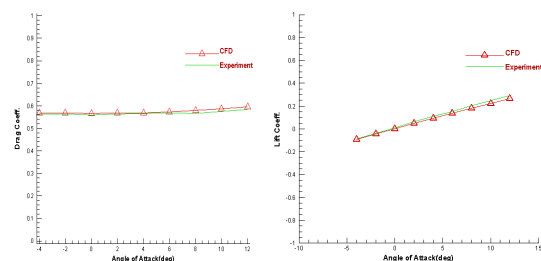


Fig. 15 Graph for Drag coeff. , lift and Pitching moment Coefficient for $r_n/r_b=0.50$ and $\theta=30^\circ$

VII. CONCLUSION

The paper describes in details the applications of AUSM scheme for different geometries and different flow regimes. AUSM scheme is suitable for lower subsonic to supersonic and even for hypersonic flows. It also captures the discontinuities and shock without oscillations. It achieves higher order accuracy by appropriate use of limiters. So this scheme work for all types of flows from lower subsonic to hypersonic flows.

REFERENCES

- [1] Liou, M.-S. and Steffen, C., "A New Flux Splitting Scheme," J. Comput. Phys., Vol. 107, 23-39, 1993.
- [2] Liou, M.-S., "A Sequel to AUSM: AUSM+," J. Comput. Phys., Vol. 129, 364-382, 1996.
- [3] Wada, Y. and Liou, M.-S., "An Accurate and Robust Flux Splitting Scheme for Shock and Contact Discontinuities," SIAM J. Scientific Computing, Vol. 18, 633-657, 1997.
- [4] Liou, M.-S., "A Sequel to AUSM, Part II: AUSM+," J. Comput. Phys., Vol. 214, 137- 170, 2006.
- [5] Edwards, J. R., Franklin, R., and Liou, M.-S., "Low-Diffusion Flux-Splitting Methods for Real Fluid Flows with Phase Transitions," AIAA J., Vol. 38, 1624-1633, 2000.
- [6] Chang, C.-H. and Liou, M.-S., "A New Approach to the Simulation of Compressible Multifluid Flows with AUSM+ Scheme," AIAA Paper 2003-4107, 16th AIAA CFD Conference, Orlando, FL, June 23-26, 2003.
- [7] Edwards, J. R. and Liou, M.-S., "Low-Diffusion Flux-Splitting Methods for Flows at All Speeds," AIAA J., Vol. 36, 1610-1617, 1998.
- [8] Kim, K. H., Kim, C., and Rho, O., "Methods for the Accurate Computations of Hypersonic Flows I. AUSMPW+ Scheme," J. Comput. Phys., Vol. 174, 38-80, 2001.
- [9] Mary, I. and Sagaut, P., "Large Eddy Simulation of Flow Around an Airfoil Near Stall," AIAA J., Vol. 40, 1139-1145, 2002.
- [10] Manoha, E., Redonnet, S., Terracol, M., and Guenaff, G., "Numerical Simulation of Aerodynamics Noise," ECCOMAS 24-28 July 2004.
- [11] Billet, G. and Louedin, O., "Adaptive Limiters for Improving the Accuracy of the MUSCL Approach for Unsteady Flows," J. Comput. Phys., Vol. 170, 161-183, 2001.
- [12] Wada, K. and Koda, J., "Instabilities of Spiral Shock – I. Onset of Wiggle Instability and its Mechanism," Monthly Notices of the Royal Astronomical Society, Vol. 349, 270-280 (11), 2004.
- [13] R. V. Chima and M. S. Liou, Comparison of the AUSM+ and H-CUSP schemes for turbo machinery applications. NASA TM-2003-212457, 2003.
- [14] M. S. Liou and C. J. Steffen, Jr. A new flux splitting scheme. *Journal of Computational Physics*, 107(1):23-39, 1993.
- [15] Herald E. Addy Jr. Glenn Research Center, Cleveland, Ohio" Ice accretions and icing effect for modern airfoil" NASA/TP-2000-310021
- [16] Bertrand Girard "wind tunnel test of DERV-ISL reference models at supersonic speed(Series ISLPWT-1) August 1997 DERV-TM-9704.(Report)

- [17] Jubaraj Sahu “Numerical computations of dynamic derivatives of finned projectile using time accurate CFD method. AIAA 2007-6581(Conference paper)
- [18] Robert L. Calloway, Nancy H. White. Measured and Predicted Shock Shapes and Aerodynamic Coefficients for Blunted Cones at Incidence in Air at Mach 5.9. NASA Technical Paper 1652, 1980.
- [19] Menter, F.R. “Zonal Two Equation $k-\omega$ Turbulence Models for Aerodynamic Flows”. AIAA 24th Fluid Dynamics conference, 6-9 July 1993: 93- 2906.
- [20] Turbulence Modeling for CFD by David C. Wilcox (book on turbulence)
- [21] A. Jameson, W. Schmidt, and E. Turkel. Numerical Solution of the Euler Equations by Finite Volume Methods Using Runge-Kutta Time-Stepping Schemes. Technical Report AIAA-81-1259, AIAA 14th Fluid and Plasma Dynamics Conference, Palo Alto, California, June 1981.(conference paper).